Electronic Supplementary Information

Enzymatic photosynthesis of formate from carbon dioxide coupled with highly efficient photoelectrochemical regeneration of nicotinamide cofactors

Dong Heon Nam,[+a] Su Keun Kuk,[+a] Hyunjun Choe,[b] Sumi Lee,[b] Jong Wan Ko,[a] Eun Jin Son,[a] Eun-Gyu Choi,[b] Yong Hwan Kim[b] and Chan Beum Park*[a]

[a] Department of Materials Science and Engineering, Korea Advanced Institute of Science and Technology (KAIST), 335 Science Road, Daejeon 305-701, Republic of Korea. E-mail: parkcb@kaist.ac.kr. [b] School of Energy and Chemical Engineering, Ulsan National Institute of Science and Technology, UNIST-gil 50, Ulsan 689-798, Republic of Korea. [+] These authors contributed equally to this work.

Materials: All chemicals were purchased from Sigma-Aldrich (St. Louis, MO) in reagent grade purity. The rhodium (III)-based electron mediator (**M** = $[Cp^*Rh(bpy)H_2O]^+$, Cp* = C_5Me_5, bpy = 2,2'-bipyridine) was synthesized according to the method reported previously.[1] *Ts*FDH was prepared as previously described,[2] and imidazole was removed from the enzyme solution using a 50 kDa molecular weight cut-off spin column (Amicon, Ireland) to prevent its inhibitory effect on **M**.

Synthesis of Co-Pi deposited hematite: The hematite was prepared via a simple solution-based method and two-step annealing.[3] First, a starting material was grown on substrate (fluorine-doped, tin-oxide-coated glass) at 100 °C in aqueous solution containing ferric chloride (0.15 M $FeCl_3 \cdot 6H_2O$) and sodium nitrate (1 M $NaNO_3$). The reactor containing the previous solution was kept in an oven for 6 h and the resultant thin film had a thickness of 371 nm, which showed the best performance in the current synthesis method. After the preparation, the substrate coated with yellow thin film was annealed via two-step annealing, with the initial annealing at 550 °C for 1 h followed by a 20-min short annealing at 800 °C. This yellow thin film turned to orange and orange-red after annealing at 550 °C and 800 °C, respectively. For deposition of Co-Pi on the surface of the hematite thin film, photo-assisted

electrodeposition was adopted.[4] The 450 W Xe lamp was used as a light source for photo-assisted electrodeposition and 0.1 M potassium phosphate buffer solution at pH 7 was used as an electrolyte. External bias (0.1 V vs. Ag/AgCl) and deposition time of 10 s were chosen as the best conditions for high activity of the hematite.

Characterization: The morphology of the hematite photoanode was observed using an S-4800 field emission scanning electron microscope (Hitachi High-Technologies Co., Japan). XRD patterns were analyzed using a powder X-ray diffractometer (Rigaku, Model D/MAX-ⅢC, Japan) under the following conditions: Cu Kα radiation, λ = 1.5418 Å; scan speed, 3 ° min^{-1}; scan range, 20-70 °. UV/Vis absorption spectra were measured using a V-650 spectrophotometer (JASCO Inc., Japan). To measure the amount of evolved oxygen, chronoamperometry was conducted in a 100 mM phosphate buffer solution (pH 7) using a three-electrode system. The oxygen concentration was continuously monitored by a calibrated fluorescence-based oxygen sensor (NEOFOX-GT, Ocean Optics, USA). All electrochemical experiments were performed with a multi-channel potentiostat/galvanostat (WMPG1000, WonATech, Korea).

NADH regeneration coupled with enzymatic formate synthesis in PEC system: For NADH regeneration, a Co-Pi/Fe_2O_3 photoelectrode was immersed in an aqueous solution at pH 13, and indium-tin-oxide-coated glass (ITO glass) was immersed in a phosphate buffer solution (5 mL, 100 mM, pH 7) containing **M** (0.25 mM) and NAD^+ (1 mM). The anodic and cathodic compartments were connected with a salt bridge, and each part was illuminated by a 450 W Xe lamp equipped with a 420 nm cut-off filter. The concentration of NADH was measured by analyzing its absorbance at 340 nm with a spectrophotometer (V-650, JASCO Inc., Japan). For the formate synthesis in the PEC cathode compartment, *Ts*FDH (10 U/mL) was added to the above-mentioned solution with continuous CO_2 injection (flow rate: 50

mL/min) during the whole reaction. High-performance liquid chromatography (LC-20A prominence, Shimadzu Co., Japan) was used to measure the concentration of formate.

Enzymatic CO_2 reduction to formate by *Ts*FDH with NADH: The enzymatic formate synthesis by *Ts*FDH was conducted in a phosphate buffer (5 mL, 100 mM, pH 7) containing NADH (0.5, 1.0, 2.0, 3.0, 5.0, 7.0, 10.0 mM) and *Ts*FDH (10 U/mL) under continuous CO_2 injection (flow rate: 50 mL/min). Note that we measured formate concentration at equilibrium state. The theoretical values of formation conversion were calculated according to the following equations. The equilibrium constant was obtained from the previous report.[5]

Henry's law: $p(CO_2) = k_H[CO_2]$, $k_H = 3.4 \times 10^{-2}$ mol/L·atm (1)

Equilibrium: $[CO_2][NADH]/[formate][NAD^+] = 420$ (2)

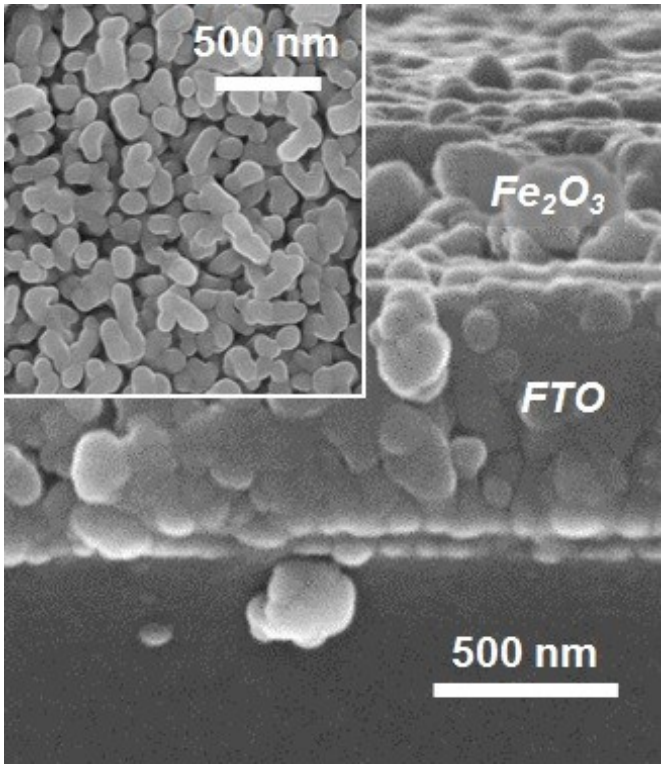

Figure S1. Cross-sectional and top view (inset) SEM images of bare hematite, exhibiting a worm-like morphology with 371 nm thickness. The hematite was synthesized by a simple solution-based method and two-step annealing.

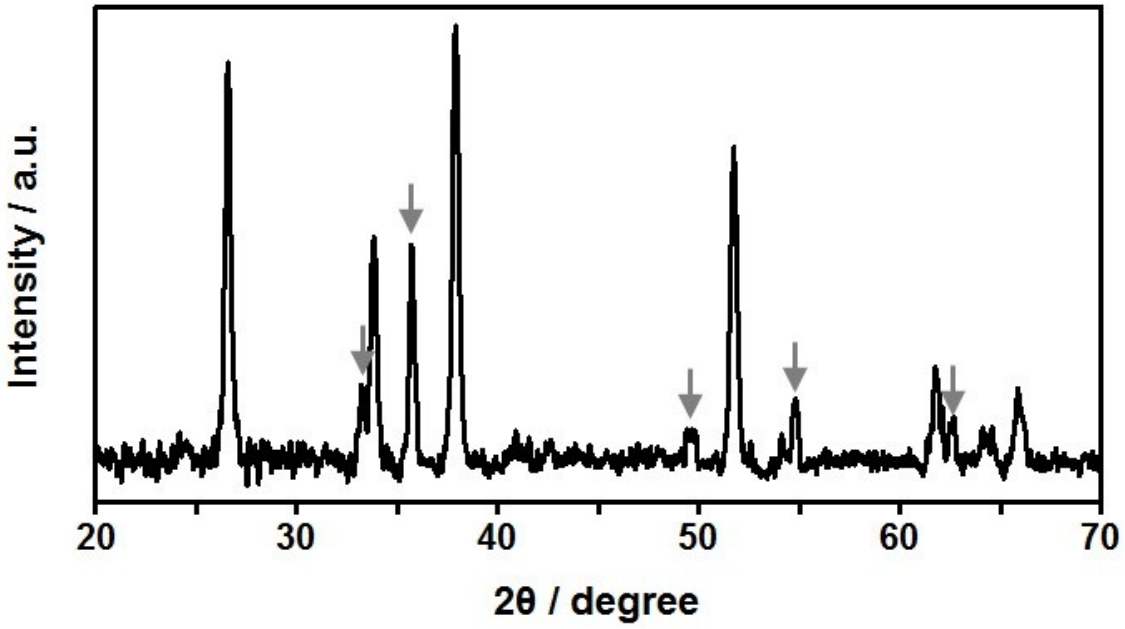

Figure S2. X-ray diffraction (XRD) pattern of hematite film synthesized on the FTO glass substrate. The XRD pattern is well matched with JCPDS #33-0664 (Fe_2O_3, marked by grey arrows) and JCPDS #46-1088 (F-SnO2).

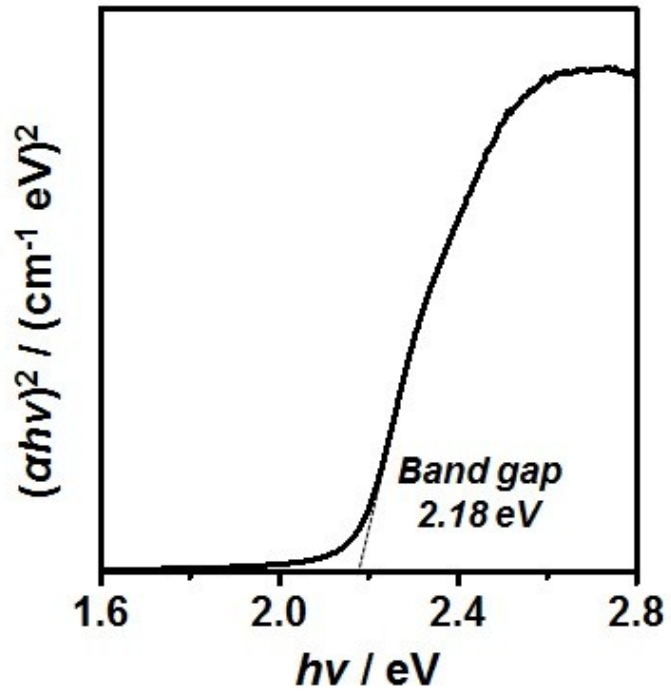

Figure S3. Plot of transformed Kubelka-Munk function versus light energy for bare hematite. From the Tauc plot, we calculated a band gap of α-Fe_2O_3 (2.18 eV), which is proper to absorb visible light. Note that we postulated that hematite has a direct band gap.

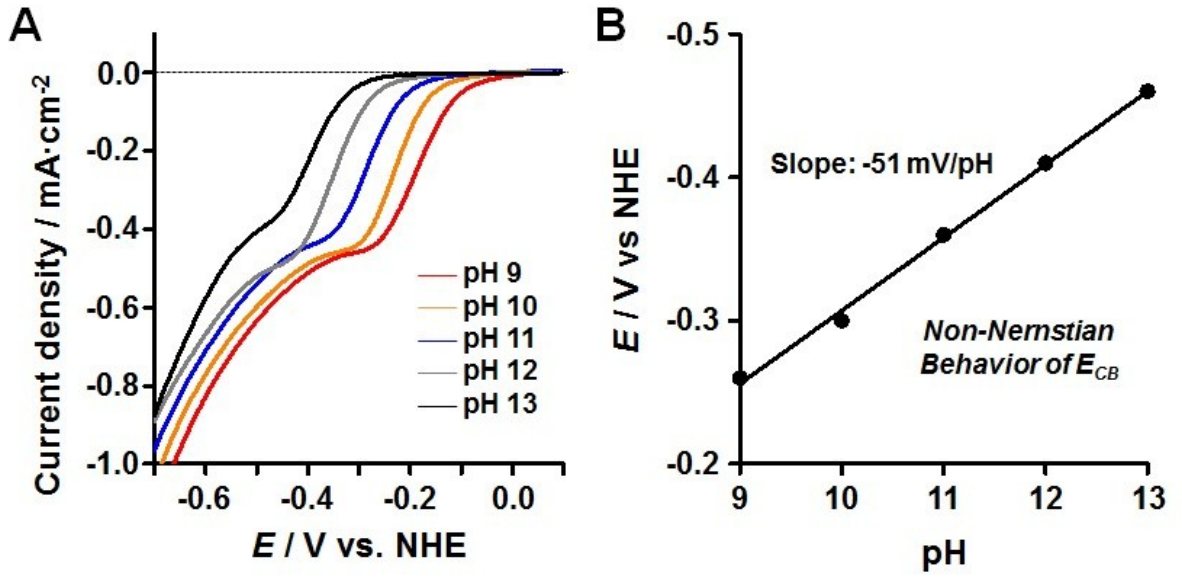

Figure S4. a) Current density-potential characteristics of bare hematite at different pH levels from 9 to 13. b) Dependence of the bare hematite conduction band (E_{CB}) on pH, showing non-Nernstian behavior with a slope -51 mV/pH. The conduction band edge of the hematite was assigned from reduction peak potentials.

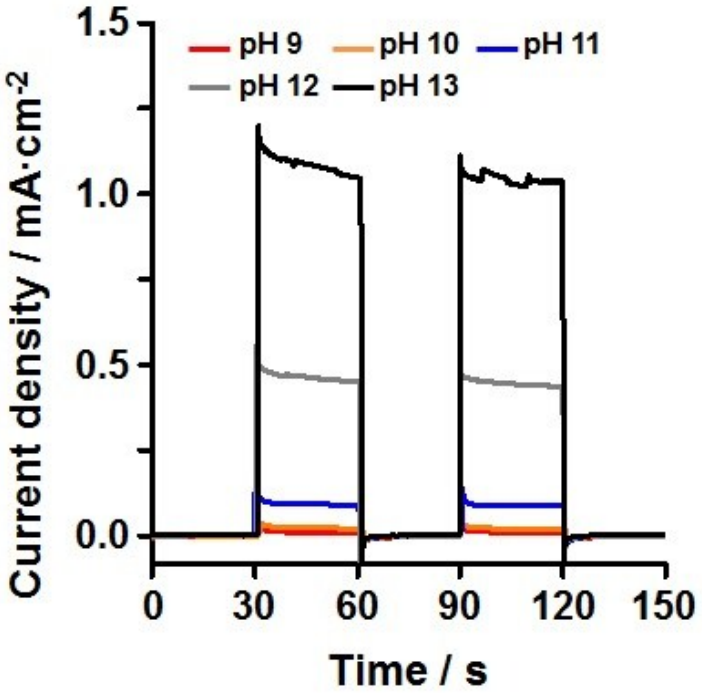

Figure S5. Under chopped light illumination, the photocurrent (0.2 V vs. Ag/AgCl) of bare hematite increased with pH, which indicates that hole transfer employing the redox shuttle ($OH^{\bullet}/OH^{-}$) led to accelerated photocatalytic water oxidation.

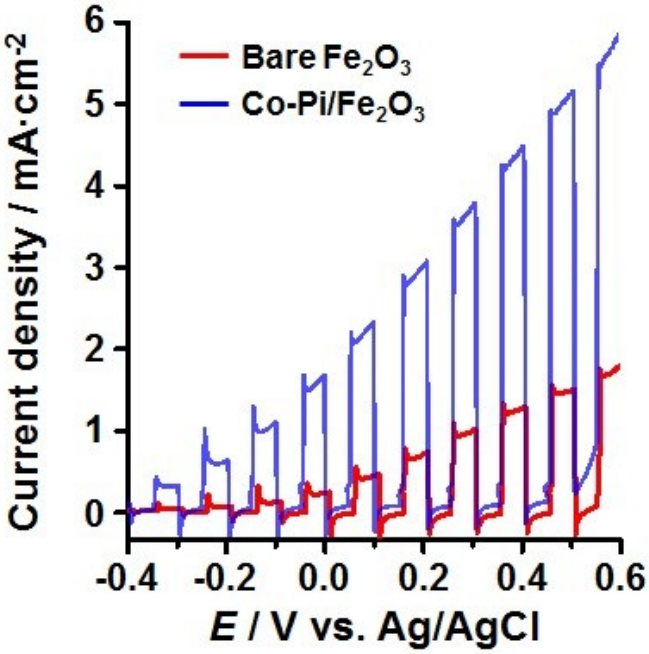

Figure S6. Current density-potential curves of hematite electrodes before (red) and after (blue) Co-Pi deposition in aqueous solution (pH 13). All experimental data measured by three-electrode system, and all electrodes have geometrical surface area of 1 cm^2.

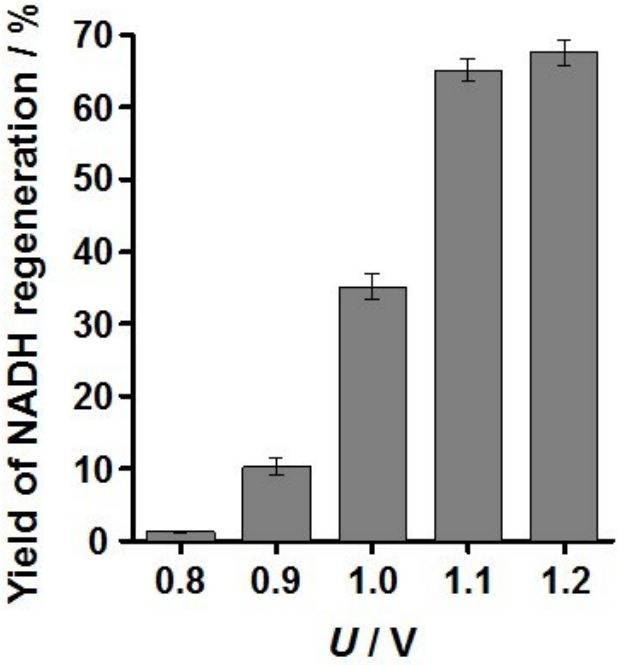

Figure S7. Dependence of NADH regeneration yield on external bias. At least 0.8 V of external bias was required to regenerate NADH due to the uncompensated solution resistance. The error bars represent standard deviation with n = 3 independent experiments at each potential.

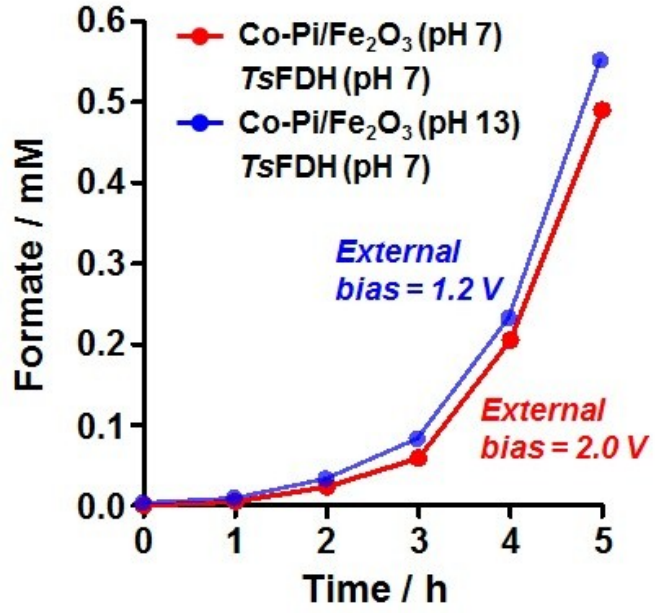

Figure S8. Time profiles of biocatalytic CO_2 reduction to formate coupled with photoelectrochemical NADH regeneration. In all the experiments, NADH regeneration and CO_2 reduction in cathodic compartment were performed in a phosphate buffer solution (pH 7.0, 100 mM), while photocatalytic water oxidation in anodic compartment was performed either at pH 13 or pH 7. All the electrodes had a geometrical surface area of 1 cm^2.

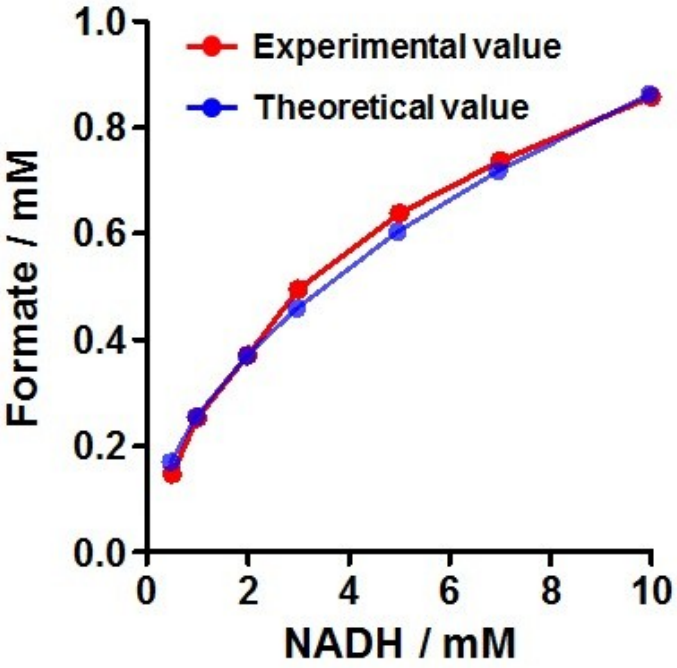

Figure S9. The change of formate concentration as a function of NADH concentration under continuous CO_2 injection. Note that we measured the formate concentration at equilibrium state. The enzymatic formate synthesis by *Ts*FDH was conducted in a phosphate buffer (100 mM, pH 7) containing NADH (0.5, 1.0, 2.0, 3.0, 5.0, 7.0, 10.0 mM) and *Ts*FDH (10 U/mL) under continuous CO_2 injection (flow rate: 50 mL/min).

References for ESI

1 F. Hollmann, B. Witholt and A. Schmid, *J. Mol. Catal. B: Enzym.*, 2002, **19–20**, 167.

2 H. Choe, J. C. Joo, D. H. Cho, M. H. Kim, S. H. Lee, K. D. Jung and Y. H. Kim, *PLoS One*, 2014, **9**, e103111.

3 L. Vayssieres, N. Beermann, S.-E. Lindquist and A. Hagfeldt, *Chem. Mater.*, 2001, **13**, 233.

4 D. K. Zhong, M. Cornuz, K. Sivula, M. Grätzel and D. R. Gamelin, *Energy Environ. Sci.*, 2011, **4**, 1759.

5 U. Rusching, U. Müller, P. Willnow and T. Höpner, *Eur. J. Biochem.*, 1976, **70**, 325.